PREDICTING FRACTURE IN ALUMINIUM WELDMENTS

U. Graf, D. Kosteas *

A calculation model for fatigue fracture of welded aluminium structures is developed and assessed by comparison with fatigue tests. The model is based on the differences of the the crack closure behaviour of small and long cracks. In the very short crack regime - crack length below grain size - crack closure is negligable. It develops in the range up to 2 mm to values measured for long cracks. The crack initiation and the early short crack growth stage are less significant. Therefore high stress concentration factors in combination with high stress gradients are not as severe as would be expected from stress or strain based concepts.

INTRODUCTION

Fracture mechanics methods together with numerical computations and measurements of the stress state in the hot spot areas of structures are used commonly to evaluate the fatigue strength of structural components. Changes of the geometry and other parameters, e.g. weld quality, R-ratio, etc., can be simulated with these methods. Problems may arise from the realistic modelling of the crack growth behaviour in the crack initiation and short crack region.

Fracture mechanics calculation model

Early investigations on the crack initiation life N_I by Grosskreutz (4) with notched and unnotched base material specimens showed a crack initiation time below 10 % of the total life N_B, Fig. 1, for surface cracks

* Chair for Steel Structures, Technical University Munich, FRG

with a visible surface length of $2a_I$ < 60 µm. For smaller cracks a value of 5% and less was detected. This is in good agreement with new data from the aluminium alloys 5083, 6082 and 7020 for smooth specimens. This test data confirmed the fact, that the short crack life part increases with increasing total life or decreasing stress range. Below a surface crack length $2a_I$ of about 60 µm the crack grows fast. In this region, the crack develops in a single grain (median grain diameters are usually between 50-100 µm for aluminium alloys). The main part of the total life of the tested small specimens is spent in the medium short crack region below 1-2 mm. For larger components the short crack part decreases and the long crack part increases up to values of 10 to 70 % of the total fatigue life depending on the geometry and stress state (1).

Based on the crack initiation data and more detailed investigations with high strength aluminium alloys and steels by Lankford (5,6), the crack initiation period can be neglected in relation to the crack propagation part, if the assumed initial crack size for the calculation is equal to the crack initiating defect. For 'defect free' base and heat affected zone (HAZ) material cracks usually originate at hard inclusions of 10-40 µm in diameter. In sound welds oxides of 20-300 µm length act as initiation sites in the hot spot area, the surface or near surface region at the weld toe. For these values the crack initiation period lies below 1 to 5 % of the total life.

The sensivity of the crack propagation behaviour to the crack size is shown in Fig. 2,3 (5,7). In the short crack range the crack growth differs from the behaviour of long crack with a irregular curvature. The changes depend on different parameters. One significant parameter is the crack length in relation to grain size or depending on material other metallurgical size factors as the distance between the perlite-bands for steels. Therefore Miller (8) established the subdivision in metallurgical short cracks (MSC), physical short cracks (PSC), and physical long cracks (PLC). This subdivision was based on the different behaviour in these three regions. The MSC-region reaches up to one or two grain diameters and is dominated by the metallurgical features of the material. The crack front lies within one or in the late stage within some grains. The transition PSC-PLC is defined by the transition of the short crack growth curve into the long crack curve. Typical values are in the region of 2 mm (9). The short crack growth behaviour depends on the crack length, the

area microcracks may be initiated in different grains with a high density, James and Morris (13).

The linear relationship between COR and the logarithmic crack length can also be expressed in terms of log(ΔK). Using this crack closure model, the growth behaviour of cracks emanating from small defects is determined by the crack length a_{MSC} at the transition MSC-PSC, and a_{PSC} at the transition to the long crack behaviour PSC-PLC. The resulting crack growth behaviour is shown in Fig. 5. Crack arrest (curve II, Fig. 5), commonly detected for short cracks in steel and aluminium, follows from the fast increase of COR and/or the described grain boundary blockage.

The fatigue crack growth behaviour in the different zones of welded joints of the alloys 5083, 6082 and 7020 is discussed in (9,14-18). The effective crack growth behaviour is independent of the parameters alloy, heat treatment (welded zone) and the stress ratio. These parameters only influence crack closure behaviour. The test data showed, that for best fit the crack growth curve as well as the crack opening curve of aluminium alloys have to be described with a multislope curve, Fig. 5. This behaviour is also apparent in high strength alloys as 7075 and 2024. The different slopes result from changes of the microscopic and macroscopic fracture mechanisms.

Assessing the fatigue strength

The described model for crack propagation behaviour was used to evaluate the influence of the different model parameters on fatigue behaviour. For the first calculations a simple rectangular specimen with a half elliptical surface crack with a fixed aspect ratio a/c of 0.95 was used. K was calculated for the maximum depth location and was used as input for the crack growth calculation. In a second stage two tested structural details, stiffener and cover plate, Fig. 8 (1-3) were analysed. The fatigue tests with these details showed that cracks start at the weld toe and develop as long surface cracks. For long surface cracks a two-dimensional analysis is sufficient for determining the stress distribution. The calculation of the stress intensity factors follows the method of Albrecht and Yamada (19) using the stress distribution in the uncracked detail. The computed stress distribution was calibrated with the measured hot spot stresses to reduce the differences between test and calculation. This leads to an increase

geometric and loading parameters as shown in Fig. 1-3. Lankfort (5) has shown that MSC-cracks grow much faster than PSC- or PLC-cracks, Fig. 2. This is also indicated by Fig. 1. As shown by Zeghloul and Petit (10) for the 7075 alloy the effective crack growth data for long cracks and the MSC-data is similar. This implies that crack closure is reduced in the MSC-region to insignificant values (9,10). This was also derived by Herman et.al. (11) with K_{max} = const., K-decreasing tests for aluminium alloys and steels. In the PSC-re- gion the closure values increase with increasing crack length up to the long crack values.

The crack opening behaviour, described by the crack opening rate COR = $\Delta K_{eff}/\Delta K$, can be modelled as shown in Fig. 4. In the MSC-region the crack is fully open during the stress cycle, COR = 1. A possible explanation are residual tension stresses in single grains promoting crack initiation and reducing crack closure. During the PSC-region closure builds up with increasing crack length. The main part of the restrain by crack closure takes place in the first 0.5 - 1.0 mm behind the crack front. Up to 2 - 4 mm another slight increase of the crack closure level is visible. Another effect is the concentration of the closure in the near surface regions of the crack (17). For half-elliptical cracks a reduction of the closure level of 20 % at the midway crack front in comparison to the surface was measured by Fleck et.al. (12). The effect is also apparent for long through cracks, if the surface layer is removed COR increases. With increasing crack length the COR is decreasing again to the former value.

Data on crack closure development and mechanisms is still too poor to predict the behaviour exactly. Tests and further investigations on the development of COR in the MSC region are in progress. As a rough estimation a linear relationship between the logarithmic crack length and COR was choosen for the model.

Another effect shown in Fig. 2 is that the crack growth speed is reduced substantially, when the crack approaches the grain boundary. In some cases it may be blocked. Grain boundary blockage was reported early for different metals (4). It results from different mechanisms, as the change of crack propagation direction (different lattice orientation in the grains) and modus (crystallographic-noncrystallographic), increasing crack closure in the grain boundary area, etc. The effect is not visible for all cracks and therefore it can be neglected, based on the knowledge, that in the hot spot

of the calculated stress levels for the cover plate detail D2. The crack growth data and the closure data are taken from (15).

The crack growth behaviour of elliptical surface cracks is computed for two stress ranges in Fig. 6. The corresponding S-N-curve, Fig. 7, is based on computations of 8 stress levels. The curves resulting from the model are denoted by MSC-PSC. The transition crack length a_{PSC} from physical short to long crack behaviour is one significant parameter. The total life is gradually reduced with increasing a_{PSC} as well as with a_{MSC}. The fatigue limit is changed significantly with a_{PSC}. The ΔK_{eff}-curve is the lower limit for the fatigue curve, because the ΔK_{eff} - crack growth curve is the upper limit growth curve for the material. The ΔK_{eff}-da/dN-curve is extrapolated from the measured data into the threshold region. It is assumed that the effective da/dN-curve has no threshold limit. The measured behaviour showed, that the existance of a threshold value for the effective da/dN-curve is questionable and if it exists, it would lie significantly lower than for the nominal da/dN-curve. Therefore the effective S-N-curve has no fatigue limit and depends only on the initial defect size and the geometry.

With the nominal crack growth behaviour and an initial crack length a_I of 10 µm for base material, the fatigue limit would lie above 300 N/mm² for a usually measured lower limit threshold stress intensity factor of 1.5 - 2 MPa√m for the stress ratio R = 0. This is too high in comparison to fatigue test data. With the proposed model the fatigue limit is reduced to realistic values.

The crack growth behaviour for a long surface crack at the weld toe of the stiffener, detail B, is shown in Fig. 9. For the lower stress range the curves reach the threshold region for $a=a_{PSC}$. The corresponding fatigue life is above 10^7 cycles. The S-N curves, Fig. 9, are limited by the ΔK (upper limit) and the ΔK_{eff}-curves (lower limit). The nominal crack growth data leads to about 50 % higher strength values in comparison to the effektive curve with a fatigue limit of 100 N/mm² at $3 \cdot 10^5$ cycles. This unusual fatigue limit - fatigue tests with specimens show fatigue limits in the region of 10^7 cycles - result from the relatively high threshold crack growth values of the tested long crack CT and SEN specimens. As stated above and shown in Fig. 9, this is corrected by the model.

Increasing the initial crack length a_i from the standard value 50 µm to 100 µm leads to a reduction in strength of about 20 %. This effect is observed in fatigue tests with variable inclusion sizes or surface roughness. Apart from the stress raising effect of notches and residual stresses, the initial crack size is a significant factor for the strength reduction in welds

The increase of the weld toe radius r_t from 0.1 mm to 1 mm leads only to a very small increase in fatigue life. The curves are overlapping. This is the results of the high crack growth rate in the MSC- and the lower part of the PSC-region and leads to negligible fatigue life portions for this region. Therefore high stress concentration factors in combination with high stress gradients, as observed for small toe radii, are not as severe as expected from local stress-strain concepts. The influence of the toe radius on the stress distribution is only significant up to a limited surface depth. Therefore the influence of the toe radius is not significant if the differences of the stress fields are limited to the MSC or the lower part of the PSC-region.

This was also detected in fatigue tests with milled weldlike shapes by Usami, Kusumoto (20). The fatigue strength was not significantly influenced by the toe radius. As a result Peterson and Neuber introduced empirical "micro support" factors into local stress-strain concepts for assessing the fatigue strength of notched specimens. The given micro support factor of 0.5 mm for aluminium is in the range between a_{MSC} and a_{PSC}. It reduces the calculated stress concentration factor to values existing in a depth approximately equal to the micro support factor below the surface of the notch. Therefore it has a similar effect on the calculated fatigue strength as the proposed short crack correction model.

In Fig. 11 and 12 the calculated S-N-curves are compared to the actual fatigue behaviour for detail B and D2. The model shows a good correlation to test data for both details. The calculated fatigue limit is relatively high. It can be reduced by increasing a_{PSC}. Further work is in progress leading to more detailed information on crack growth and closure behaviour in the short crack regime and reducing the existing uncertainties for the parameters of the model.

Summary and Conclusion

A fracture mechanics calculation model for fatigue fracture based on the crack closure behaviour in the short crack region was discussed and applied to structural details.

Literature data and additional investigations showed, that the crack initiation life part is neglectable, if the initial crack length a_i, at the transition from crack initiation to crack propagation, is set equal to the real crack initiation defect. The resulting a_i - values of 10 - 200 µm for 'defect free' welded aluminium components lay in the short crack range. The crack growth behaviour of short cracks differs from the long crack behaviour significantly, leading to problems in predicting the behaviour. The proposed model simulate the short crack behaviour on the base of the development of the crack closure and the effective growth behaviour. First calculations with the model show a good correlation with fatigue tests.

The parameters of the model are based on the poor available data and have to be varified in further work. Other open points of interest are the influence of residual stresses, the irregular growth behaviour in the HAZ of the 7020-alloy, and the behaviour in the threshold regime below 10^{-9} m/cycle.

References

(1) Kosteas, D., Poalas, K., Bericht des Lehrstuhls für Stahlbau Nr. 120, München, 1986.
(2) Kosteas, D., Proc. Int. Conf. on Fatigue of Welded Constructions, The Welding Institute, Abington, Cambridge, 1987.
(3) Graf, U., Kosteas, D., Poalas, K., Proc. 3. Int. Con. Aluminium Weldments III, München, 1985.
(4) Grosskreutz, J.C., ASTM STP 495, 1971, p 5-60.
(5) Lankford, J., Fatigue of Engineering Materials and Structures 6(1983)1, p 15-31.
(6) Lankford, J., Engineering Fracture Mechanics 9(1977), p 617-624.
(7) Leis, B.N., Forte, T.P., ASTM STP 743, 1981, p 100-124.
(8) Miller,K.J., Proc. ECF 6, Amsterdam, 1986, p 2149-2167.
(9) Graf, U., Kosteas, D., 19. Sitzung DVM AK Bruchvorgänge, Freiburg, 1987, p 251-261.
(10) Zeghloul, A., Petit, J., Fatigue Fract. Engng.

Mater. Structures 8(1985)4, p 341-348.
(11) Herman, W.A., Hertzberg, R.W., Jaccard, R., J. Fatigue and Fracture Eng. Mat. Struc. (1987)7.
(12) Fleck, N.A. et. al., J. Fatigue and Fracture Eng. Mat. Struc. 6(1983)3.
(13) Morris, L.M., James, M.R., ASTM STP 811, p 179-206.
(14) Kosteas, D., Poalas, K., Bericht des Lehrstuhl für Stahlbau Nr. 124, München, 1987.
(15) Kosteas, D., Graf, U., Bericht des Lehrstuhl für Stahlbau Nr. 109, TU München, 1984.
(16) Graf, U., Kosteas, D., IIW-Doc.XIII-1241-87 Part I
(17) Graf, U., Kosteas, D., IIW Doc.XIII-1241-87 Part II
(18) Graf, U., Kosteas, D., Welding Research, '85 ASM's Int. Welding Cong., Toronto, 1985, p 123-130.
(19) Albrecht, P., Yammada, K., J. Structural Devision, ASCE, 103(1977), p 337-389
(20) Usami, S., Kusumoto, S., Trans. JWS 9(1978)1, p 8-16.

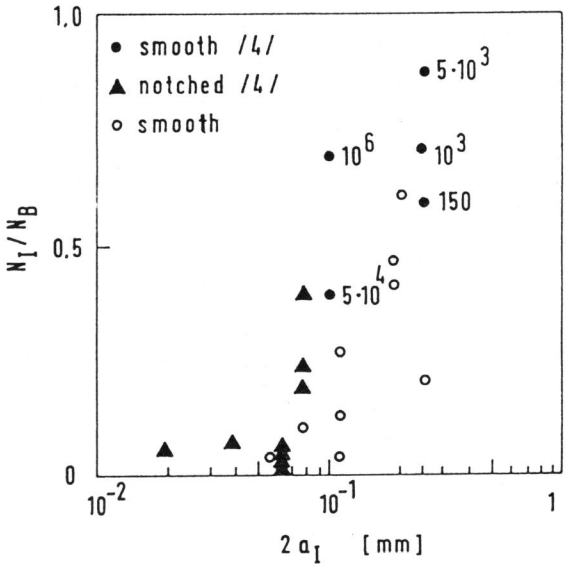

Figure 1 Surface crack length $2a_I$ in relation to the crack initiation life N_I to total life N_B fraction for medium strength aluminium alloys.

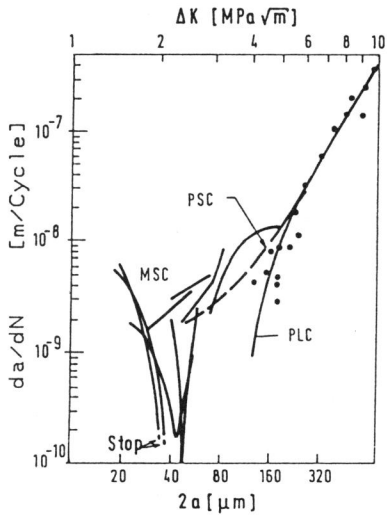

Figure 2 Short crack behaviour 7075-alloy, smooth specimen (5)

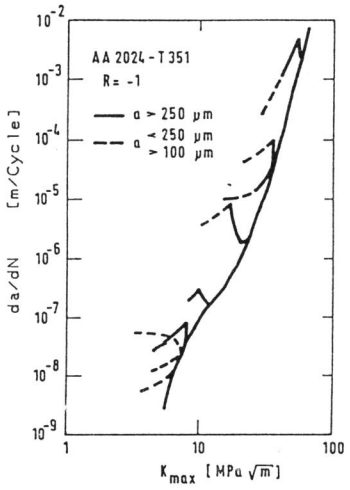

Figure 3 Short crack behaviour 2024-alloy, crack from notch (7)

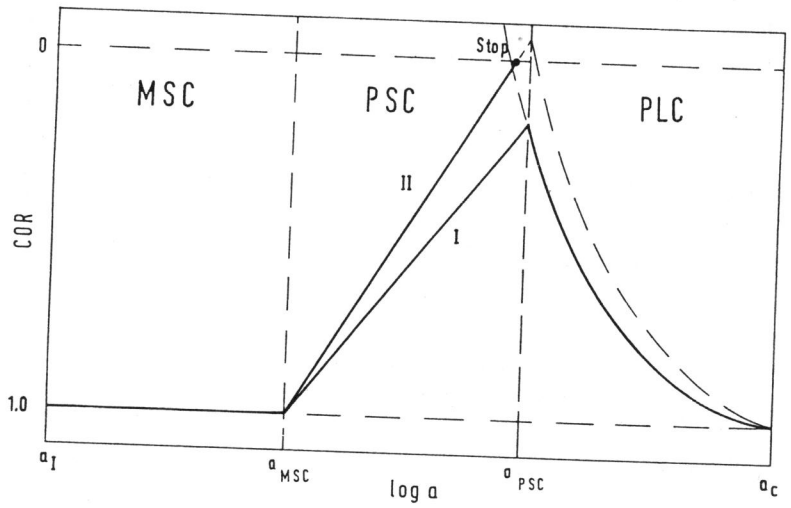

Figure 4 Model for the development of the crack opening rate (COR) with the crack length

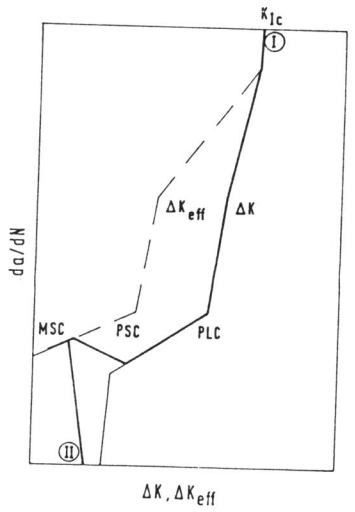

Figure 5 Systematic crack growth behaviour based on the model of Figure 4

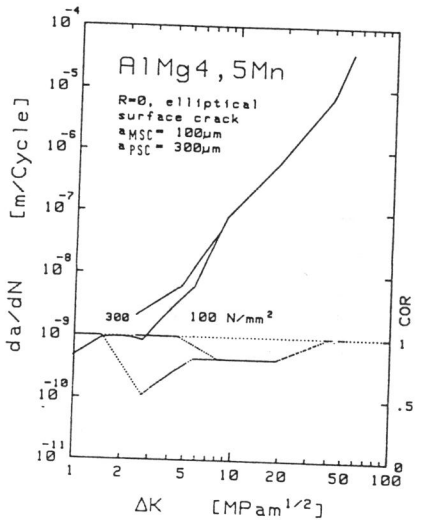

Figure 6 Crack growth behaviour for two stress ranges, semielliptical crack, a_I=10µm

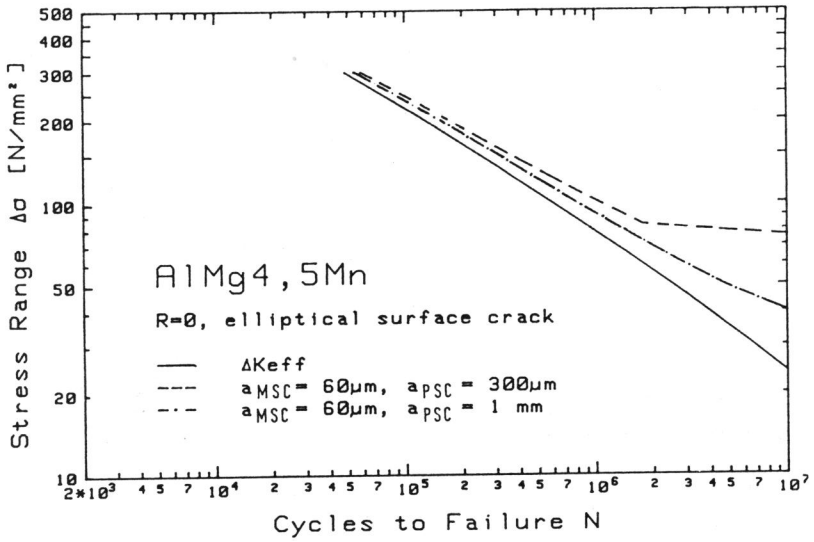

Figure 7 Calculated S-N-curve for different a_{PSC}-values, a_I = 10 µm

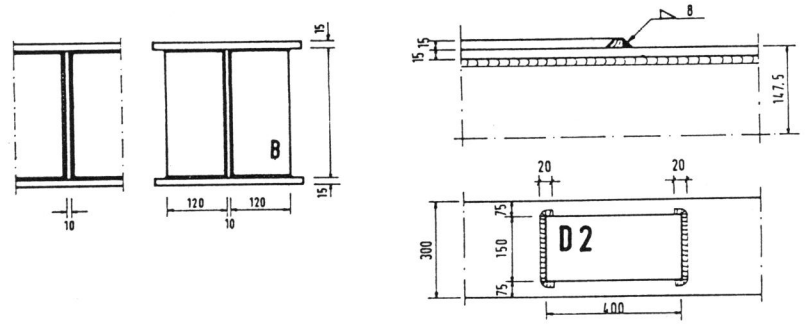

Figure 8 Geometry of the stiffener (B) and the cover plate detail (D2)

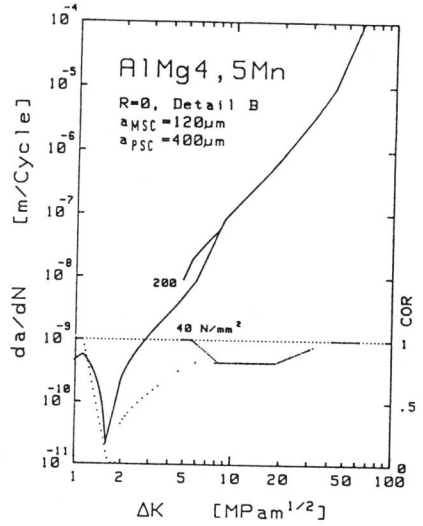

Figure 9 Crack growth behaviour, Detail B, a_I = 100 µm

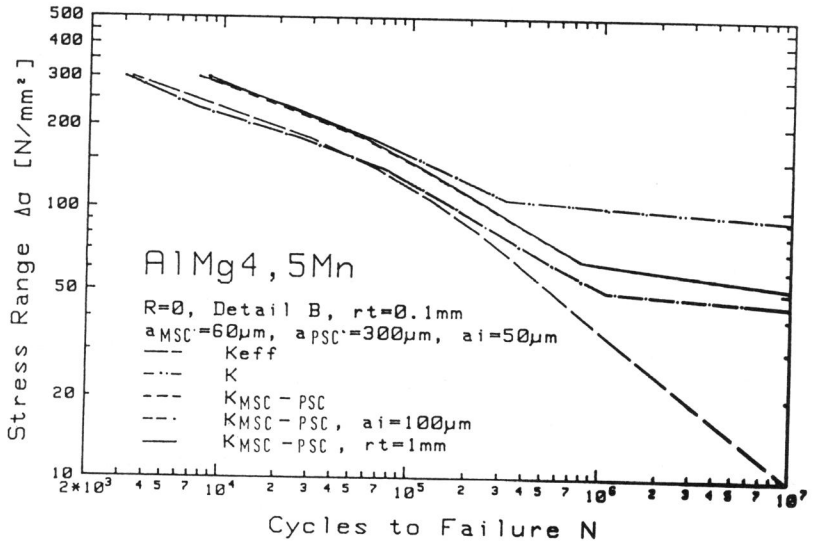

Figure 10 Calculated S-N-curves for **Detail B**

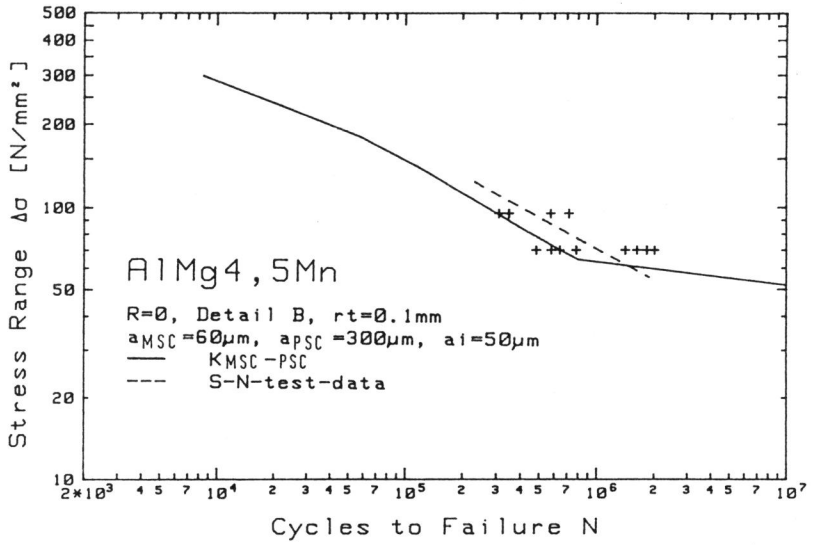

Figure 11 Comparison of the calculated S-N-Curve and test data (R=+0.1) for Detail B

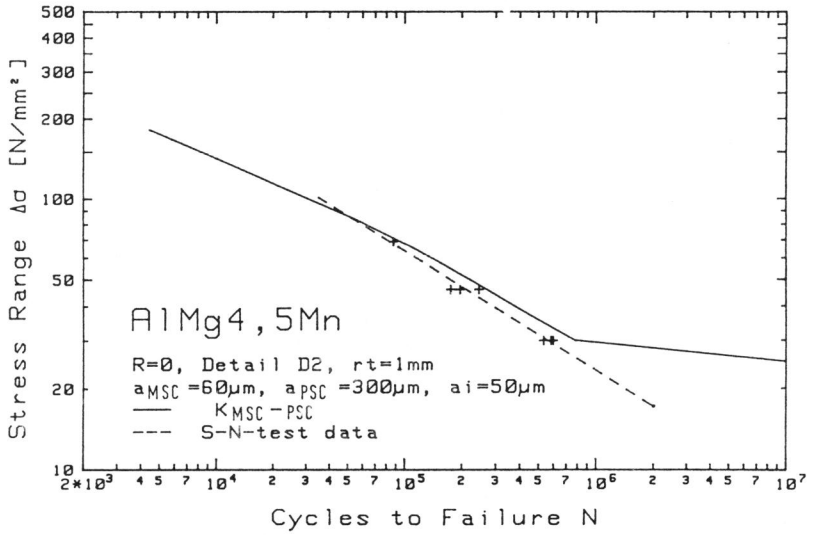

Figure 12 Comparison of the calculated S-N-Curve and test data (R=+0.1) for Detail D2